5012–5028 *Nucleic Acids Research, 2018, Vol. 46, No. 10* *Published online 20 March 2018*
doi: 10.1093/nar/gky209

Transcriptional and epigenetic adaptation of maize chromosomes in Oat-Maize addition lines

Zhaobin Dong[1,2,†], Juan Yu[3,†], Hui Li[1], Wei Huang[1], Ling Xu[1,2], Yue Zhao[1], Tao Zhang[4], Wenying Xu[3], Jiming Jiang[4,5], Zhen Su[3,*] and Weiwei Jin[1,*]

[1]National Maize Improvement Center, Key Laboratory of Crop Heterosis and Utilization, the Ministry of Education, Key Laboratory of Crop Genetic Improvement, Beijing Municipality, Center for Crop Functional Genomics and Molecular Breeding, College of Agronomy and Biotechnology, China Agricultural University, Beijing 10093, P. R. China, [2]Plant Gene Expression Center, U.S. Department of Agriculture-Agricultural Research Service, Plant and Microbial Biology Department, University of California at Berkeley, CA 94710, USA, [3]State Key Laboratory of Plant Physiology and Biochemistry, College of Biological Sciences, China Agricultural University, Beijing 10093, P. R. China, [4]Department of Horticulture, University of Wisconsin-Madison, Madison, WI 53706, USA and [5]Department of Plant Biology, Department of Horticulture, Michigan State University, East Lansing, MI 48824 USA

Received January 09, 2018; Revised March 08, 2018; Editorial Decision March 10, 2018; Accepted March 13, 2018

ABSTRACT

By putting heterologous genomic regulatory systems into contact, chromosome addition lines derived from interspecific or intergeneric crosses allow the investigation of transcriptional regulation in new genomic environments. Here, we report the transcriptional and epigenetic adaptation of stably inherited alien maize chromosomes in two oat–maize addition (OMA) lines. We found that the majority of maize genes displayed maize-specific transcription in the oat genomic environment. Nevertheless, a quarter of the expressed genes encoded by the two maize chromosomes were differentially expressed genes (DEGs). Notably, highly conserved orthologs were more severely differentially expressed in OMAs than less conserved orthologs. Additionally, syntenic genes and highly abundant genes were overrepresented among DEGs. Gene suppression was more common than activation among the DEGs; however, the genes in the former maize pericentromere, which expanded to become the new centromere in OMAs, were activated. Histone modifications (H3K4me3, H3K9ac and H3K27me3) were consistent with these transcriptome results. We expect that *cis* regulation is responsible for unchanged expression in OMA versus maize; and *trans* regulation is the predominant mechanism behind DEGs. The genome interaction identified here reveals the important consequences of interspecific/intergeneric crosses and potential mechanisms of plant evolution when genomic environments interact.

INTRODUCTION

Polyploidy arises from either unreduced gametes (resulting in autopolyploids) or interspecific crosses (resulting in allopolyploids), allowing it to be amongst the most pivotal forces in species evolution (1,2). Compared with animals, plants, especially flowering plants (angiosperms), are highly tolerant of interspecific crosses. Thus, plants are excellent models to investigate the interaction of formerly separate genomic environments during interspecific hybridization (3). Plant interspecific crosses may overcome fertilization barriers, resulting in allopolyploids or haploids (1,4). In allopolyploids, the genomes from both parental gametes are merged, whereas in haploids one parental genome is eliminated after fertilization (5,6). Some rare hybridization events can result in chromosome addition lines, which are in-between allopolyploids and haploids in genome interaction. Chromosome addition lines are usually rescued and maintained deliberately after interspecific crosses; they contain a complete set of uniparental chromosomes with one or more pairs of stably inherited chromosomes from the alien parent (7–12).

In interspecific hybrids, such as allopolyploids and chromosome addition lines, the transcriptional regulatory mechanisms from two genomic environments interact, leading to widespread gene expression changes. The

*To whom correspondence should be addressed. Tel: +86 10 62734909; Fax: +86 10 62734909; Email: weiweijin@cau.edu.cn
Correspondence may also be addressed to Zhen Su. Email: zhensu@cau.edu.cn
†The authors wish it to be known that, in their opinion, the first two authors should be regarded as Joint First Authors.
Present address: Juan Yu, Institute of Biophysics, Chinese Academy of Sciences, Beijing 100101, P. R. China.
Disclaimer: The funders had no role in study design, data collection and analysis, decision to publish or preparation of the manuscript.

transcriptional changes observed in interspecific hybrids are likely caused by two types of regulatory mechanisms: *cis*-regulatory elements and *trans*-regulatory factors. The *cis*-regulatory elements include gene expression enhancers and promoter sequences that influence gene expression and mRNA stability of downstream genes (13–15). *Trans*-regulatory factors, such as transcription factors (TFs), either act independently or coordinate with *cis* elements throughout the hybrid genome (14–17). Previous studies on gene transcription in interspecies hybrids from fruit flies, yeast, tomato and *Arabidopsis* have shown *cis*- and/or *trans*-dependent transcriptional regulation of parental orthologs (14–16,18). In addition, comparison of *cis*- versus *trans*-regulatory effects has revealed that *cis*-regulatory factors predominate the observed transcriptional divergence of parental orthologs (14). *Trans*-regulatory factors are commonly associated with *cis* regulation, when they are involved in selfing sibling and environmental responses (15,16). Compared with allopolyploids where the two parental genomes interact, chromosome addition lines facilitate precise regulation studies because only a small subset of the donor genome (one or just a few chromosomes) interacts with the receptor genome, reducing the complexity of possible genomic interactions. Chromosome addition lines have been developed from several animal and plant species (7–10,12,19,20). However, the regulatory mechanism underlying the widespread gene transcription of the alien chromosome(s) is still unclear. As far as we know, only two previous reports investigated chromosome-wide gene expression in chromosome addition lines (8,21). Using an Affymetrix Barley1 GeneChip, Cho *et al*. characterized barley-specific gene transcription in wheat–barley chromosome addition lines; however, because of the limited accuracy of chip technology, quantification of the gene transcription was difficult (21). Wilson *et al*. took advantage of an animal chromosome addition line, a mouse hepatocyte strain introgressed by human chromosome 21, to compare TF binding sites, chromatin modification, and gene expression between mice and human (8). They found that the majority of orthologous pairs were transcriptionally and epigenetically inherited from their respective parents, indicating that a regulatory DNA sequence, rather than any other species-specific *trans* factor, may determine the interspecific divergence in gene expression (8). Recent advances in next generation sequencing for profiling gene regulation may provide a more precise understanding of expression regulation mechanisms compared to previous work with microarrays.

Rines and Phillips have developed a series of oat-maize addition (OMA) lines by a sexual cross between oat (*Avena sativa* L., 2n = 6x = 42) and maize (*Zea mays* L., 2n = 20), resulting in the addition of individual maize chromosomes to the complete oat genome (11,19,20). The allohexaploid oat genome originated itself from a hybridization between an diploid 'D genome' and a tetraploid 'AC genome' (22–24). OMA lines set up an interesting situation as four diverged genomic regions are present, hence the additional orthologous maize genes will exist in four copies (A, C, D and maize) versus three copies in oat (A, C and D). This artificial 'quadruple hybrid' may mimic natural interspecific hybridization, providing an ideal model to investigate the mechanisms underlying alien chromosome survival and genomic adaptation in the recipient genomic environment. We therefore conducted RNA-seq (RNA sequencing) and examined three histone modifications using chromatin immunoprecipitation sequencing (ChIP-seq) in the OMA lines containing maize chromosome 6 (Chr6) or chromosome 9 (Chr9). The reads that were uniquely mapped to the maize genome but not to the oat transcriptome were used to profile the maize gene expression in native and recipient genomic environments. We found that many alien maize genes showed similar expression levels in oat genomic environment compared to the maize parental genomic environment. However, 26–28% of the alien maize genes were differentially expressed in the OMA lines, indicating that *cis* effects may dominate the regulation of alien maize gene expression. Notably, we observed a negative correlation between coding sequence conservation and expression level. Syntenic genes were over-represented amongst differentially expressed genes (DEGs) but non-syntenic genes were not. In contrast to the chromosome-wide suppression of alien maize DEGs, several genes in the newly expanded centromere of the OMA lines were activated. These results suggest that centromeric transcriptional activation may contribute to stabilizing the centromeres in interspecific/intergeneric hybrids. Furthermore, our histone modification analysis in the OMA lines support the transcriptional profiling results, implying that *cis* and *trans* mechanisms may synergistically regulate alien gene transcription and facilitate alien gene survival in an interspecific/intergeneric genome.

MATERIALS AND METHODS

Plant materials

The oat cultivar Starter and all the oat–maize addition lines, including the two OMA lines with B73 as the maize donor (OMA6.33 and OMA9.41) (20) and the two OMA lines with Seneca60 as the maize donor (OMAd6.1 and OMAd9.1) (19) were kindly provided by Drs Howard W. Rines and Ronald L. Phillips (University of Minnesota, USA). All seeds were germinated and grown in a growth chamber at 28°C for 16 h of light and at 20°C for 8 h of darkness.

GISH and FISH

Genomic *in situ* hybridization (GISH) was conducted as previously described with minor modifications (25). Maize genomic DNA was labeled with digoxigenin–11-dUTP or biotin–11-dUTP (Roche) via nick translation. The digoxigenin- and biotin-labeled probes were incubated with anti-digoxigenin antibody conjugated with rhodamine (Roche) and anti-avidin antibody conjugated with fluorescein isothiocyanate (Vector Laboratories), respectively. Chromosomes were counterstained with 4′, 6-diamidino-2-phenylindole (DAPI) in an anti-fade solution. Fluorescence *in situ* hybridization (FISH) analyses on root tip chromosomes were performed according to procedures as previously described (26,27). Slides were also counterstained with 4′, 6-diamino-phenylindole (Vector Laboratories). An epifluorescence microscope (Olympus BX61) attached to a

CCD camera (QImaging; RETGA-SRV FAST 1394) was used to capture FISH/GISH images. Image-Pro Plus 6.0 software (Media Cybernetics) was used to analyze and adjust all digital images.

RNA extraction and RNA-seq

Total RNA from leaves was isolated from maize, oat and OMA lines at 14 and 40 days after planting (DAP). Leaves from at least 6 individual plants were pooled together as one biological replicate and then grinded in liquid nitrogen. Three biological replicates of ∼100 mg tissue powder were used to extract and purify RNA through RNAprep pure (for plant) Kit (Tiangen, Beijing, China; #DP432) according to the instruction manual. The construction of an RNA-seq library was performed according to the standard manufacturer's protocol in the Illumina TruSeq RNA Sample Preparation Kit v2 (cat#RS-122-2001); this generated 100 base pair-end reads on the Illumina HiSeq2000 platform.

ChIP and ChIP-seq

ChIP was performed as previously described by Du *et al.* (28). Histone modification antibodies against H3 trimethyl-K4 (ChIP grade, ab8580; Abcam [Hong Kong] Ltd.), acetyl-K9 (ChIP grade, ab10812; Abcam [Hong Kong] Ltd.) and trimethyl-K27 (ChIP grade, Upstate Biotechnology [Millipore 07-449, Temecula]) were used for this ChIP experiment. Nuclei were isolated from ∼10 g of fresh leaf tissue and digested with micrococcal nuclease (Sigma-Aldrich). Quantitative ChIP-PCR was performed to determine the relative enrichment of modified histone-associated sequences in the bound fraction over the mock control. We used actin gene as a positive control for H3K4me3 and H3K9ac to normalize the enrichment of each negative amplicon when using the primers, Os5S-F/R and Quinta-LTR-3F/R, respectively. The actin gene was a negative control for H3K27me3. The primers, B6-7F/R and B9-9F/R, were used as positive controls for ChIP-qPCR (Supplementary Table S1). Both ChIP DNA and mock DNA were used for the preparation of a high-throughput sequencing library, including end repair, adaptor ligation, size selection and polymerase chain reaction (PCR) amplification, followed by Illumina Hiseq2000 sequencing (Berry Genomics Co., Ltd).

Quantitative RT–PCR

Quantitative RT-PCR was performed as described previously (29). Three biological replicates and three technical replicates were performed for each genotype. Oat and maize actin homolog genes were used as internal references to normalize expression data by using a pair of primers with identical sequence matches from both species (Forward: CCAC GTACAACTCCATCAT, Reverse: CCGATCCAGACA CTGTACTTCC). For all other gene primers, only maize-specific primers were selected for qRT–PCR (Supplementary Table S1). Relative expression levels were calculated as $2^{-\Delta\Delta Ct}$, and the standard deviation was calculated among three biological replicates.

Estimate on the relative transcriptome size (RTS)

For isolation of the total nucleic acids (TNA), maize B73 or OMA leaf blade was harvested at 14 DAP and ground to fine powder in liquid nitrogen. A total of 100 mg tissue powder was mixed vigorously in 500 μl extraction buffer (250 mM Tris HCl, pH8.5; 375 mM NaCl; 25 mM ethylenediaminetetraacetic acid (EDTA); 1% sodium dodecyl sulphate; 1% 2-mercaptoethanol). The resulting tissue homogenate was centrifuged at 12 000 rpm for 10 min to pellet insoluble debris, and the supernatant was transferred to another tube. In the supernatant, 0.3 ml Phenol B and 0.3 ml chloroform were added, and the solution was mixed thoroughly by vortex. The mixture was kept on ice for 15 min and then centrifuged at 12 000 rpm for 15 min. One volume of ice cold isopropanol was added to the supernatant and the solution was mixed well, then centrifuged at max speed for 15 minu. The DNA/RNA pellet was washed with 70% ethanol by three times, and then re-suspended in RNase-free H2O/0.1% EDTA, pH = 8.0. A total of 4 μg TNA were used for reverse transcription following the instruction of M-MLV First Strand Kit (Invitrogene, Cat no. C28025-032). cDNA specific primers were designed as at least one primer of each pair included exon junctions. Genomic DNA-specific primers were designed based on the intergenic region. All the primer sequences are listed in the Supplementary Table S1. The estimate of RTS was calculated as described by Coate and Doyle (30).

RNA-seq data analysis

RNA-seq was performed for B73, Seneca60 maize lines, OMA6.33, OMA9.41, OMAd6.1, OMAd9.1 lines and oat Starter as parallel tests. For the maize lines, the pair-end reads were mapped to the reference genome of maize B73 version 3 using a TopHat tool with default parameters (31); The duplicated reads mapped to more than one location in the genome were filtered, and only the uniquely mapped tags were retained. For the additional lines, we constructed a new assembly as a reference, which consisted of oat transcriptome assembled by Trinity (32) and B73 single chromosome 6 or chromosome 9 genome sequence. Only the reads uniquely mapped on Chr6 or Chr9 were selected and then normalized with the reference for B73 Chr6 or Chr9. Fragments per kilobase million (FPKM) value by Cufflinks tool was used to measure differences in gene expression levels between B73 and additional lines (33). FPKM value for the OMA samples was then re-normalized and re-calculated by multiply the RTS of OMA relative to maize in order to counteract the transcriptome size bias. DEGs were identified by the cutoff with absolute value of $\log_2$ fold change > 0.8 and a P-value < 0.05. A GO analysis for the functional categorization of DEGs was performed using AgriGO (34), with maize genes from Chr6 or Chr9 as reference background instead of whole genome genes. Sequence similarities were analyzed with BLAST (35), using maize genes against the assembled oat transcriptome as well as public expressed sequence tag (EST) sequences from NCBI. The oat transcript assigned with the highest bit score of each maize gene was defined as the closest corresponding ortholog.

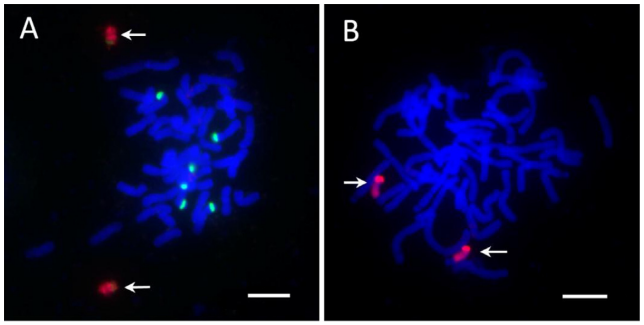

Figure 1. Cytological characterization of OMA6 and OMA9. (**A**) The two copies of maize Chr6 in OMA6 were detected by FISH and GISH using 45S rDNA (green) and maize genomic DNA (red) as probes, respectively. (**B**) GISH signals (red) in an OMA9 root tip cell after using maize genomic DNA as the probe represent the maize chromosome pairs. Bars = 10 μm.

ChIP-seq data analysis

Single-end ChIP-seq and input reads were mapped to the reference accordingly same as that in the RNA-seq analysis using Bowtie2 (36), allowing one base mismatch with default parameters, and only uniquely mapped reads were used for further analysis. The MACS (37) program was used to identify peaks and convert the data to bigwig/wig format with default parameters. The data was all normalized based on their sequencing depth before following analysis. The visualization of the ChIP-seq tags over selected genomic regions were created by Integrative Genomics Viewer (38). To compare the modification level in maize and OMA for all genes, we calculated the average ChIP-seq enrichment across 3 kb upstream and downstream of the TSS by CEAS (39). A heatmap plot of *z*-score was created to illustrate the average histone modification markers in the gene promoters. Boxplots used to compare the histone modification level for up- and downregulated genes were performed by R package. The statistical significance between the OMA and B73 was calculated using a Wilcoxon signed-rank test.

RESULTS

Maize chromosome transmission is stable in OMA6 and OMA9

OMA lines, OMA6.33 and OMA9.41 contain introgressed maize B73 chromosomes within the Starter oat genomic background (20). To confirm the genomic stability of OMA6.33 and OMA9.41 (which are simplified as OMA6 and OMA9, respectively, in the remaining text), we used GISH and FISH to analyze the cytogenetic characteristics of the OMA lines. After one generation of seed bulking, all of the randomly selected progeny (at least 10 individuals descended from both OMA6 and OMA9) showed a disomic addition of maize chromosomes in OMA6 and OMA9 (2n = 42 + 2). Figure 1 shows that probes specific maize genomic sequences identified a pair of maize Chr6 in the OMA6 (Figure 1A) and Chr9 in the OMA9 (Figure 1B) by GISH. Maize 45S ribosomal DNA (rDNA) is located on maize Chr6. Thus, FISH revealed two 45S rDNA signals on the short arm of the maize chromosome in the OMA6 and six 45S rDNA loci in the remaining hexaploid oat chromosomes, as expected (Figure 1A). These results are consistent with previous studies, which identified maize chromosome transmission by molecular marker-based genotyping of OMA lines (20), suggesting the stable inheritance of alien genomic material in the OMA lines used in this study.

Transcriptional response of maize genes to oat genomic environment

To investigate transcriptional regulation, we examined whole leaf blades of seedling at 14 days after planting (DAP) from maize B73, OMA6, OMA9 and oat Starter by RNA-seq. In total, 71.0 M, 56.2 M 59.1 M and 99.5 M high quality 100 bp paired-end reads were generated from the B73, OMA6, OMA9 and oat Starter, respectively (Supplementary Table S2). Three biological replicates were used for the B73, OMA6 and OMA9 and four for the oat Starter. Reads from B73 were mapped to the maize B73 genome by using TopHat (31). To accurately align the OMA reads, we had to distinguish oat reads from maize transcripts. Because an assembled oat genome is unavailable, we used the Trinity software to *de novo* assemble an oat transcriptome from our four biological replicates of Starter RNA-seq (32). The assembled oat transcriptome contained 14 068 transcript contigs with an average transcript length of 1184 bp and an N50 value of 1452 bp (Supplementary Table S3). The OMA6 and OMA9 reads were then mapped to the assembled oat transcriptome and the maize Chr6 or Chr9 sequence, with a strict alignment requirement of only one base mismatch. The reads that mapped uniquely to the maize chromosomes, but not to the oat transcriptome, were used for further analysis. This strategy substantially reduces the chance of oat transcripts being mapped mistakenly to the maize chromosomes. To evaluate the accuracy of this mapping strategy, we counted the number of reads aligned to both the maize chromosomes and the oat transcriptome: (i) for the three replicates of OMA6, the proportions of such reads were only 0.063, 0.066 and 0.055%; for the three replicates of OMA9, the proportions were only 0.029, 0.025 and 0.028%, indicating that very few maize reads were eliminated mistakenly because of multiple alignments; (ii) for the three replicates of maize B73, only 0.07, 0.068 and 0.069% of the mapped reads were aligned to the oat transcriptome (Supplementary Table S4). Thus, our mapping strategy may efficiently differentiate maize from oat transcripts, and allowed further analysis of gene expression specifically originating from the alien maize chromosomes. In total, maize-specific reads comprised 12.3% of reads pairs in OMA6 and 8.8% in OMA9 (Supplementary Table S2). Therefore, approximately one tenth of each OMA transcriptome originated from a maize chromosome, similar to the endogenous maize chromosome's contribution to the native maize transcriptome. After alignment, the maize Chr6- and Chr9-specific reads from B73 and the corresponding OMA lines were extracted and then normalized to the Chr6 and Chr9 references, respectively, and the FPKM was determined. We thus generated a chromosome-wide transcript profile for the B73 maize, OMA6 and OMA9. Compared with B73 gene expression, we identified 595 DEGs (236 upregulated and 359 downregulated genes) and 502 DEGs (232 upregulated

and 270 downregulated genes) in the OMA6 and OMA9, respectively (Supplementary Table S5).

Transcriptome analysis after adjusting transcriptome size

An assumption for RNA-seq analysis is that the compared transcriptomes should have equal size (called 'transcriptome normalization'). In this study, we noticed possible differences in transcriptome size between maize and the OMAs. To address this concern, we used a previously described strategy to calculate relative transcriptome size (RTS) (30). Briefly, total RNA and gDNA (TNA) were co-extracted from the same tissue used in our RNA-seq and reverse transcribed. Then maize cDNA- and gDNA-specific primers of randomly selected genes (Supplementary Table S1) were used in quantitative RT-PCR to quantify the gene expression based on a genome normalization. Because maize chromosome pairs in our OMA materials are stable in both individuals and generations, estimation of relative gene expression based on genome normalization should be more accurate than that based on transcriptome normalization (the RNA-seq analysis). We found that relative gene expression per genome from the qRT-PCR analysis correlated substantially with the gene expression profile from the RNA-seq analysis (Pearson correlation $R^2 = 0.93$ in OMA6 and $R^2 = 0.97$ in OMA9) (Figure 2A and B). Through a previously proposed approach (30), we divided the value of relative expression per genome from the qRT-PCR assay by the relative expression per transcriptome from the RNA-Seq dataset to calculate the RTS of maize chromosome in the OMAs relative to that in B73. The RTS was 1.033 and 1.179 in the OMA6 and OMA9, respectively (Figure 2C). These results suggest that maize chromosomes exhibit a stable relative transcriptome in OMA lines, although the genome size is quite different between maize and oat. These findings indicate that the oat genome may not significantly affect alien maize transcriptome size.

To minimize potential bias due to transcriptome size difference, we re-normalized and re-calculated FPKM for the OMA RNA-seq datasets, which was the original FPKM multiplied by the RTS of the OMA lines (1.033 for OMA6 and 1.179 for OMA9). After these adjustments, the DEG list of OMA6 remained unchanged compared with the results from the analysis without the transcriptome size adjustment, whereas for the OMA9, the number of downregulated genes was reduced by five and the upregulated genes remained unchanged compared with the original analysis (Figure 3A and B, Table 1 and Supplementary Table S6). Four genes in the OMA6 and three genes in the OMA9 were revived (extremely upregulated, FPKM = 0 in the B73 but FPKM > 5 in the OMAs); 157 genes in the OMA6 and 80 genes in the OMA9 were silenced (extremely downregulated, FPKM > 5 in the B73 but FPKM = 0 in the OMAs), accounting for ∼40% of the downregulated genes in both OMA lines (Table 1 and Supplementary Table S6). In addition, the downregulated genes in general showed a higher fold changes than the upregulated genes (Figure 3C and D), indicating that transcriptional inactivation on the alien maize chromosome appear to be predominant. In summary, the total numbers of DEGs were 595 and 497 in the OMA6 and OMA9, respectively, which, surprisingly, represented only 28.12 and 25.97% of the expressed genes on their respective chromosomes (Table 1). Therefore, the majority of the chromatin on the alien maize chromosome maintained inherent transcriptional activity. We also investigated the distribution of DEGs on the corresponding chromosome. Both the density and fold change of the DEGs varied greatly, and no obvious enrichment of the DEGs on the alien maize chromosomes was detected (Supplementary Figure S1A and B).

To confirm the DEG patterns in the alien chromosomes, we conducted RNA-seq analyses using another OMA6 and OMA9 lines (designated as OMAd6.1 and OMAd9.1 to differentiate from the B73-OMA lines), in which Seneca60 maize was used as the maize donor (11) and Seneca60 maize RNA-seq data were used as the control (Supplementary Table S2). Similar to the OMA6 and OMA9, we used whole blades of leaves at 14 DAP from OMAd6.1 and Seneca60 for RNA-seq, and we also performed RNA-seq on the 40 DAP tissues from OMAd lines and Seneca60. At 14 DAP stage, compared with the gene expression in Seneca60, 839 genes (395 upregulated and 444 downregulated genes) were identified as DEGs in the OMAd6.1 and 695 (353 upregulated and 342 downregulated genes) DEGs were identified in the OMAd9.1. At 40 DAP stages, 789 genes (399 upregulated and 390 downregulated genes) and 754 genes (381 upregulated and 373 downregulated genes) were identified as DEGs in OMAd6.1 and OMAd9.1, respectively (Figure 4A and B; Supplementary Table S7). In addition, 72 and 93 genes were silenced (FPKM > 5 in Seneca60 whereas FPKM = 0 in OMAd6.1) in the OMAd6.1 at 14 and 40 DAP, respectively, while 59 and 111 genes were silenced in the OMAd9.1 at the two stages, respectively. Few genes exhibited de-repression (FPKM = 0 in Seneca60 whereas FPKM > 5 in OMAds), 31 and 45 genes in the OMAd6.1 at 14 and 40 DAP, respectively, and 38 and 44 genes in the OMAd9.1 at the two stages, respectively (Supplementary Table S7). These results further suggest predominant suppression of genes from the alien maize chromosomes. Notably, the gene expression pattern of the B73-OMAs correlated highly with that of the Seneca60-OMAds at both DAP stages (Figure 4C and D; Supplementary Figure S2A and B). Over 67% of the DEGs in the B73-OMAs overlapped with the DEGs in the Seneca60-OMAds at 14 and 40 DAP (Figure 4C and D; Supplementary Figure S2C). We also noticed that the DEG expression patterns showed a higher correlation between developmental stages (OMAd lines at 14 DAP versus 40 DAP) than between different donor maize chromosome (OMA lines versus OMAd lines; Supplementary Figure S2A and B). These results indicate an inherent mechanism underlying gene expression regulation in the alien maize chromosome, that may not be significantly influenced by the donor maize genomic background and even more slightly by developmental stage. Nevertheless, it is notable that profound sequence diversity exists in different maize lines (40,41). Thus, mapping Seneca60 reads to the B73 genome will cause bias inevitably. In addition, Seneca60 is a hybrid stock and not an inbred, which could compromise the robustness of the conclusions on gene expression. For those reasons, we only focused on the B73-OMA dataset in the following analyses.

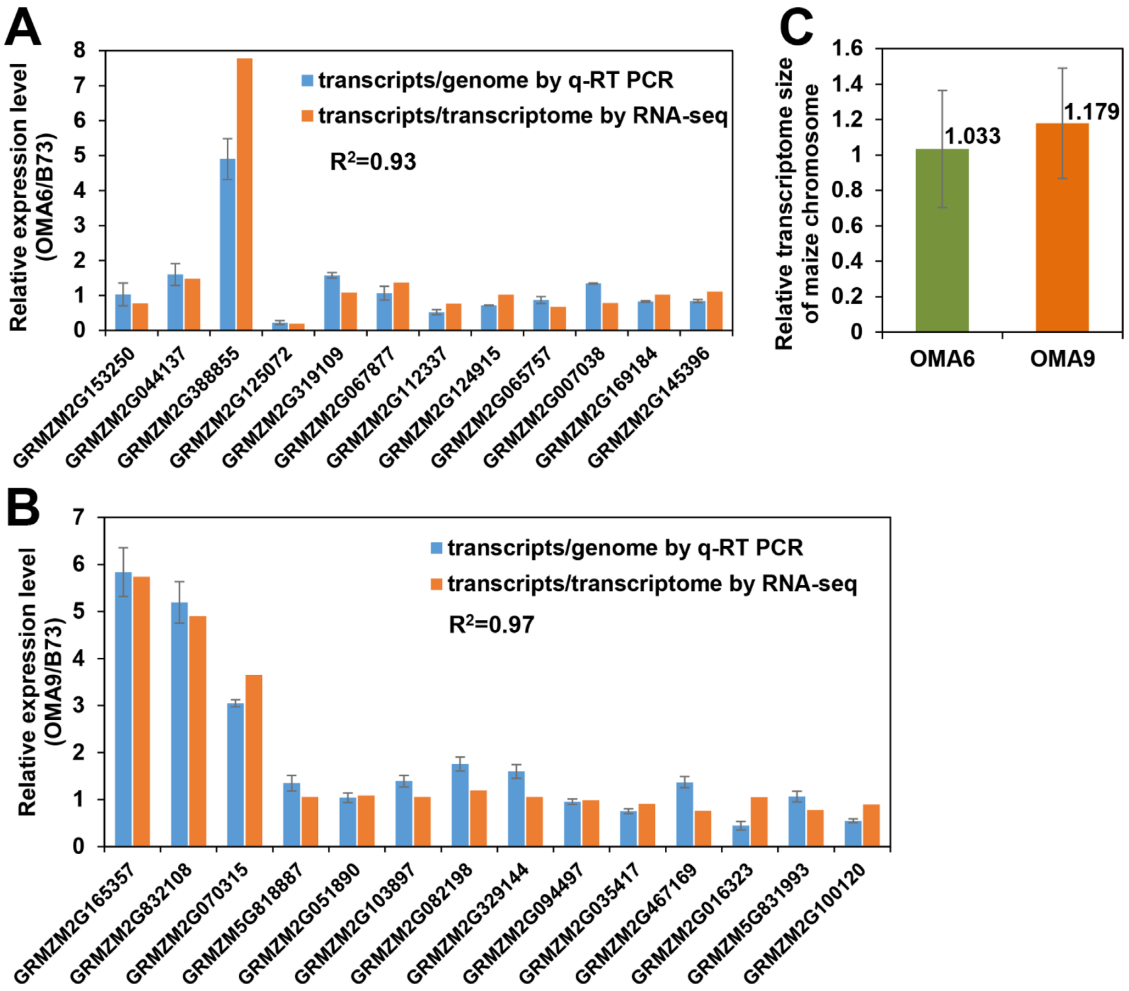

Figure 2. Comparison of the expression value estimated by RNA-seq versus qRT-PCR. (**A** and **B**) Fold change of randomly selected maize genes shows high correlation between RNA-seq and qRT-PCR for both OMA6 (A) and OMA9 (B). Results based on RNA-seq estimate transcript level per transcriptome, while qRT-PCR value estimate transcript per genome (see 'Materials and Methods' section). The value of R^2 was calculated as Pearson correlation. (**C**) Average estimate of transcriptome size of the maize chromosomes in OMA relative to the transcriptomes of the corresponding chromosomes in maize. The error bars stand for the standard deviation, $n = 12$ for OMA6 and $n = 14$ for OMA9.

Table 1. Overview of DEGs

	Total genes	Expressed genes[1]	Non-DEGs	DEGs	Upregulated	Extremely upregulated[2]	Downregulated	Extremely downregulated[3]
OMA6 versus B73	3290	2116	1521 (71.88%)	595 (28.12%)	236 (11.15%)	4 (0.19%)	359 (16.97%)	157 (7.42%)
OMA9 versus B73	3006	1914	1417 (74.03%)	497 (25.97%)	232 (12.12%)	3 (0.16%)	265 (13.85%)	80 (4.18%)

[1]Expressed genes represent the genes with FPKM > 1 in either maize or OMA.
[2]Extremely upregulated genes represent the genes showing FPKM = 0 in B73 and FPKM > 5 in OMA lines.
[3]Extremely downregulated genes represent the genes showing FPKM > 5 in B73 and FPKM = 0 in OMA lines. Values in parentheses represent the corresponding percentage of the genes relative to the expressed gene on the chromosome. DEG: Differentially expressed gene.

Functional analysis of the DEGs

To investigate the regulatory mechanisms underlying the gene expression in alien maize chromosomes, we analyzed the expected function of the DEGs. No significant functional enrichment was detected in the downregulated genes in both OMA6 and OMA9. The upregulated genes from both OMAs showed enrichment in translation-related pathways and the gene ontology of ribosome structure (Supplementary Figure S3), indicating that the additional maize and/or oat chromosomes may prefer maize components for gene translation through an unknown mechanism.

OMAs are good models to investigate C3/C4 photosynthesis because the individual C4 chromosome is included in the C3 genetic background. The gene expression lev-

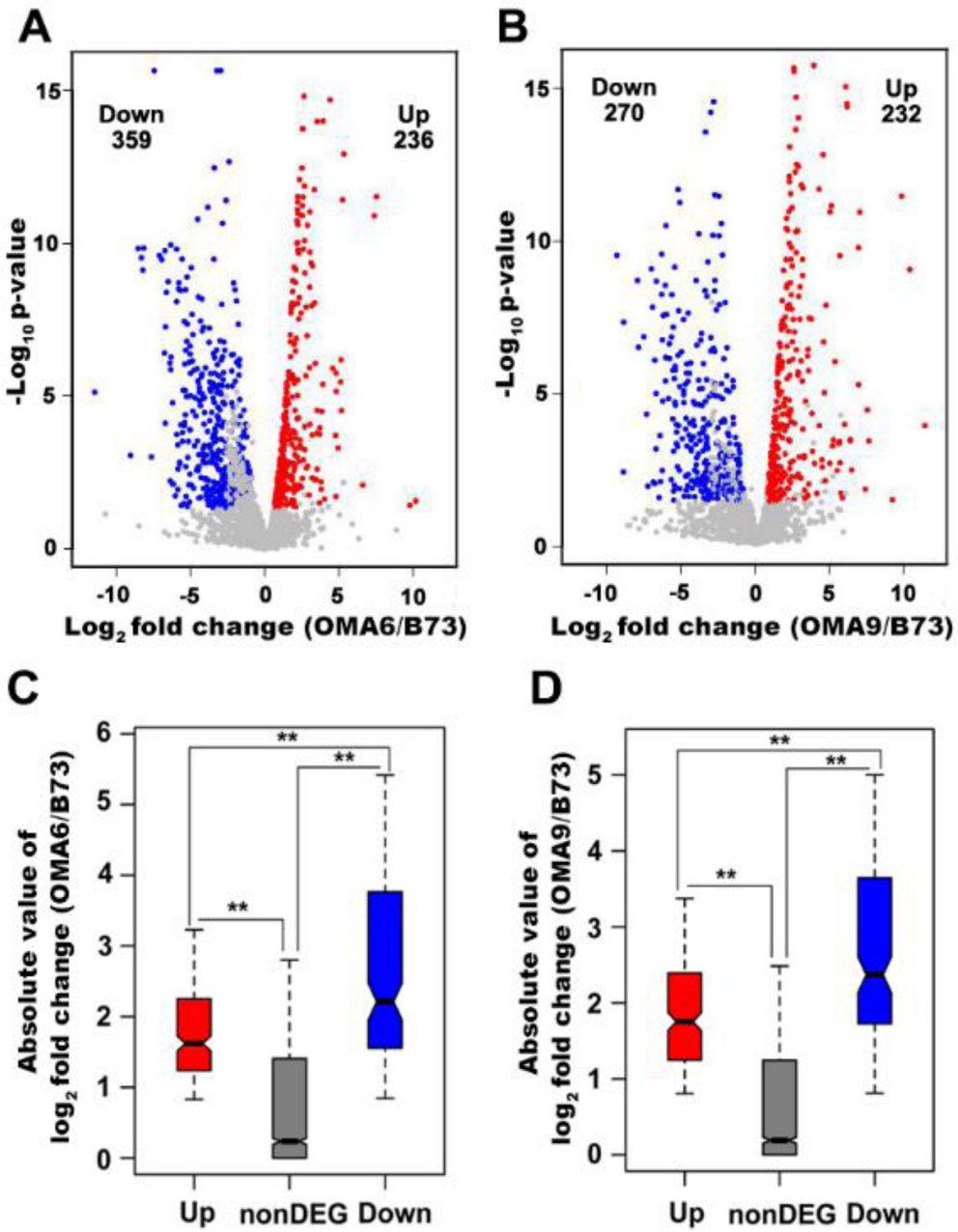

Figure 3. Quantitative profile of DEGs in B73-OMAs. (**A** and **B**) Volcano plots of DEGs in B73-OMAs. (A) OMA6. (B) OMA9. The *x*- and *y*-axes show fold changes on a $\log_2$ scale and the *P*-value on a $-\log_{10}$ scale, respectively. Upregulated genes are presented in red, and downregulated genes are presented in blue. (**C** and **D**) A comparison of the absolute value for the fold change between up- and downregulated genes in OMA6 and OMA9, respectively, relative to the non-DEGs as control; ** indicate significant differences with a *P*-value < 0.05 based on a Wilcoxon signed-rank test.

els of the two key C4 enzymes in the OMAs, pyruvate orthophosphate dikinase (PPDK) on maize Chr6 and phosphoenolpyruvate carboxylase (PEPC) on Chr9, were not significantly changed compared with those in the maize B73 (Table 2). These data are consistent with the results of previous studies investigating the RNA and protein expression of the two genes in OMAs (42,43). However, the expression of other C4-related genes was changed in the oat genomic environment. For example, dicarboxylate/tricarboxylate carriers (DTCs) and mesophyll envelope protein 3 (MEP3) were induced significantly in the OMAs, while NADP-dependent malic enzyme 2 (NADP–ME2), ribulose-phosphate 3-epimerase (RPE), fructose 1, 6-bisphosphatase (FBP) and transketolase (TKL) were all suppressed in the OMAs (Table 2). The mosaic expression pattern of the C4 genes may not support C4 photosynthesis in an oat background, and a previous report has also shown that individual maize chromosome had limited impact on C3 photosynthesis in OMA lines (43), suggesting that engineering C4 photosynthesis into C3 plants by interspecific hybridization may be challenging, since a high number of C4 related genes all through the genome need to be transferred and expressed.

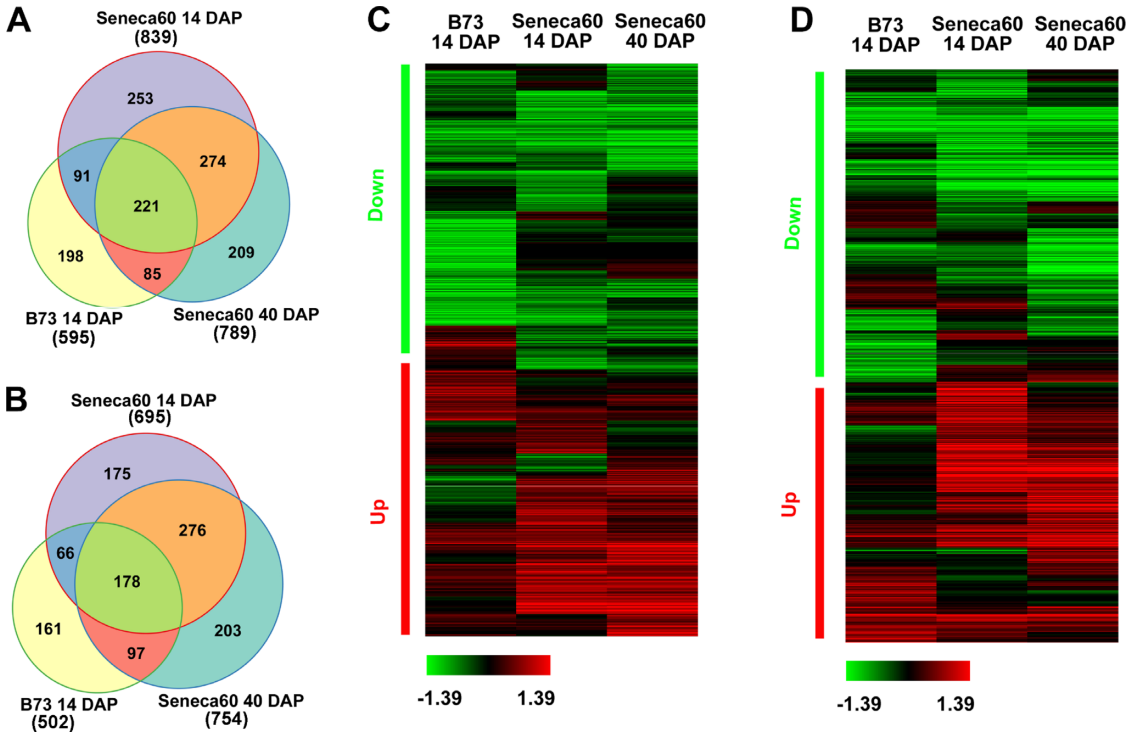

Figure 4. Correlation analysis of DEGs from different maize genetic donors at different developmental stages. (**A** and **B**) Venn diagrams of DEGs in OMA lines compare the expression effect of maize donor background (OMAd6.1 and OMAd9.1 from Seneca 60 compared with OMA6 and OMA9 from B73), as well as growth stages (14 days after planting [DAP] in comparison with 40 DAP). (**C** and **D**) Heatmap of DEGs from triple datasets. The up- and downregulated genes are well clustered together among the triple datasets. The scale of color density correlates with the $\log_2$ value of fold changes in genes.

Table 2. Gene expression profiles of essential enzymes involved in the C3/C4 photosynthesis pathway

Gene ID	Chr	Gene name	RPKM B73	RPKM OMA	$\log_2$ fold change	Significant
GRMZM2G042146	6	C4.BS.Dicarboxylate/tricarboxylate Carrier (DTC)	81.6226	330.889	2.01931	yes
GRMZM2G051630	6	C4.BS.Dicarboxylate/tricarboxylate Carrier (DTC)	114.177	668.431	2.54951	yes
GRMZM2G178960	9	C4.BS.Ribulose-phosphate 3-epimerase (RPE)	68.8523	0.509308	−7.07882	yes
GRMZM2G034061	9	C4.ME.Sugar Transporter	135.722	6.55578	−4.37174	yes
GRMZM2G095287	9	C4.BS.Fructose 1,6-bisphosphatase (FBP)	294.421	45.6077	−2.69053	yes
GRMZM2G033208	9	C4.BS.Transketolase (TKL)	2506.97	659.44	−1.92663	yes
GRMZM2G122479	6	NADP-dependent malic enzyme2 (NADP-ME2)	139.482	40.698	−1.77705	yes
GRMZM2G083841	9	C4.ME.Phosphoenopyruvate Carboxylase(PEPC)	14530.2	6304.05	−1.2047	no
GRMZM2G306345	6	C4.ME.Pyruvate Orthophosphodikinase (PPDK)	45916.8	43263.5	−0.08587	no
GRMZM2G089136	6	C4.ME.Phosphoglycerate Kinase (PGK)	4541.57	5980.62	0.39710	no
GRMZM2G305851	6	C4.ME.Envelope Protein (MEP3)	136.964	380.601	1.47449	yes

TFs control transcriptional dynamics and play critical roles in almost all biological processes (44). Of the 213 TFs in OMA6, 34 (16.0%) were downregulated and 11 (5.2%) were upregulated; of the 172 TFs in OMA9, 18 (10.5%) were downregulated and 17 (9.9%) were upregulated (Supplementary Table S8). The low percentage of differentially expressed TFs (DETFs), indicates that TFs in OMA lines are not more likely to undergo differential expression than any other gene category. In the OMA6, the number of downregulated TFs was substantially higher than that of the upregulated TFs, further suggesting that alien maize genes are predominantly suppressed in oat genomic environment. Of the 21 TF families containing DETFs in the OMA6 and OMA9, only three (MYB-related, NAC and Co-Like) showed consistent changes in the OMA6 and OMA9; five TF families (HB-other, ERF, WRKY, bHLH and GRAS) including DETFs changed in an opposite direction in the OMA6 and OMA9 (Supplementary Figure S4), indicating that TF functional changes may not contribute uniformly to the transcriptional response of alien maize chromosome to the oat genomic environment in OMAs.

DEGs show high sequence similarity in the orthologous maize–oat gene pairs

In addition to cellular regulatory mechanisms, such as TFs and epigenetic modifications, genetic sequence characteristics can also regulate transcription (8). We examined the association between genetic sequence characteristics and gene expression level in the OMA lines. To avoid potential bias from pseudogenes or tissue-specific silenced genes, we excluded maize non-expressed genes (FPKM < 1 in both the

maize B73 and the OMA lines) in the following analyses. Expressed alien maize genes (FPKM > 1 in either the B73 or the OMA lines) without significantly changed expression levels were defined as non-DEGs. We aligned the coding sequences of all maize expressed genes on the two maize chromosomes to the oat reference database, which included the oat transcriptome developed in our current study and the publicly available expressed sequence tag (EST) sequences retrieved from the NCBI database. For each maize gene query, oat transcript contigs or EST hits with the highest bit score generated by the Basic Local Alignment Search Tool (BLAST) were identified as the oat corresponding ortholog. Of the 2116 and 1914 expressed genes on the respective maize Chr6 and Chr9, we identified 1168 and 1031 maize-oat orthologous gene pairs, respectively. The two sets of orthologous pairs were then divided into five classes sorted by the sequence similarity between the maize–oat orthologous pair. Each class contains the same number of orthologous pairs. Class 1 contains the orthologs with the highest maize–oat sequence similarity; Class 5 has the orthologous pairs with the lowest sequence similarity. The proportions of DEGs and non-DEGs in each class varied greatly. Notably, the proportions of the upregulated and downregulated genes in the orthologous gene pairs dropped with reduced sequence similarity between the pairs, whereas the proportions of non-DEGs increased as the with reduced similarity in both OMA lines (Figure 5A and B), indicating that a higher sequence similarity between the maize–oat orthologous pair may correlate with a stronger tendency to be differentially expressed.

We also analyzed the differential expression of the orthologous transcripts in oat by comparing the OMA lines and the oat Starter at 14 DAP using the same strategy as in the analysis of maize DEGs. At the cutoff of $P < 0.05$, 15 pairs of the orthologs in the OMA6 and 16 pairs in the OMA9 were differentially expressed for both the maize genes and the oat transcripts. Intriguingly, the fold change of oat transcripts showed a significant negative correlation with that of the maize orthologs (Figure 5C), indicating a potential dosage compensation between maize and oat orthologs with high sequence similarity.

Syntenic genes were over-represented among DEGs

During the history of evolution, flowering plants experienced multiple whole genome duplications, and thus underwent several rounds of genome fractionation (45–47). Based on synteny with the sorghum genome, genes from the maize genome have been categorized as non-syntenic or syntenic genes (47,48). About 44.50% (1464/3290) of the genes on maize Chr6 can be considered as syntenic genes and the remaining 55.50% are non-syntenic genes. To eliminate the effect from the pseudogenes, we only took the expressed genes (FPKM > 5 in either maize or OMAs) in the following analysis. Among the maize expressed genes in the OMA6, 56.20% of non-DEGs are syntenic genes; 64.22% (149/232) of the upregulated genes and 57.38% (206/359) of the downregulated genes are syntenic genes (binomial test, $P < 0.04$, Supplementary Figure S5). Similarly, syntenic genes were also over-represented among OMA9 DEGs (binomial test, $P < 0.02$; Supplementary Figure S5). However, no over-represented pattern was observed in any type of subgenome (subgenome maize1 and maize2, with or without paralogs; data not shown) (47). Although we were unable to directly evaluate syntenic gene distribution in oat and maize because of lacking an oat genome sequence, our results showing an over-representation of syntenic genes in the OMA DEGs, implying that syntenic orthologs from the alien maize chromosomes may be more susceptible to transcriptional adjustment when the maize chromosome is introduced into a closely related grass genome.

Chromosome-wide profile of histone modifications on the maize addition chromosome

To investigate the dynamic chromatin changes on the maize chromosomes, we conducted ChIP-seq assay in the OMA6, OMA9, and maize B73. Antibodies to detect the three chromatin modifications: H3K4me3, H3K9ac (H3K4me3 and H3K9ac are recognized as positive regulators of gene expression) and H3K27me3 (a negative regulator of gene expression) were used in the ChIP-seq assay (49). In total, 1076 M high quality reads were generated (Supplementary Table S9). According to the stringent mapping strategy in our RNA-seq data analysis as described above, all ChIP-seq reads of the B73 and OMA lines were screened for unique reads that were exclusively mapped to the B73 chromosomes. The Chr6- or Chr9-specific reads were then normalized (Supplementary Table S9). We examined the extent of modification at the genic region around the transcript start site (TSS) of the Filtered Gene Set on Chr6 and Chr9. Consistent with the previous characterization of the three modifications in maize (49), H3K4me3 and H3K9ac was detected in genic regions and enriched around the TSSs of genes in the B73, whereas H3K27me3 was enriched broadly across the gene body (Figure 6). These chromatin modification patterns within in the genic region of the OMAs generally resembled those in the B73 (Figure 6). In both OMA6 and OMA9, average H3K9ac levels in the Chr6 and Chr9 were reduced compared with those in the B73 (Figure 6). In contrast, H3K27me3 and H3K4me3 levels were higher in both OMA lines than in the B73 (Figure 6). These data suggest that potential gene activation from the elevated H3K4me3 may be counteracted by the inhibitory effects of reduced H3K9ac and increased H3K27me3, resulting in the observation that a majority of the maize genes in OMA lines maintain normal expression levels.

We next performed a cluster analysis on the three modifications on Chr6 and Chr9. We divided genes from each chromosome into an active group, including genes enriched for H3K4me3 and H3K9ac but lacking H3K27me3, and an inactive group, including genes with a low abundance of H3K4me3 and H3K9ac but a high abundance of H3K27me3. For both Chr6 and Chr9 in B73, the active group contained approximately equal numbers of genes as the inactive group. In contrast, in the OMA6 and OMA9 DEGs, the active group was markedly over-represented (Figure 7A–D). Consistent with our findings by RNA-seq, the DEGs showed substantially higher FPKM values than the non-DEGs in the B73 leaves (Figure 7 E and F), suggesting that the originally active genes located in open chromatin appear to be more differentially expressed in OMAs.

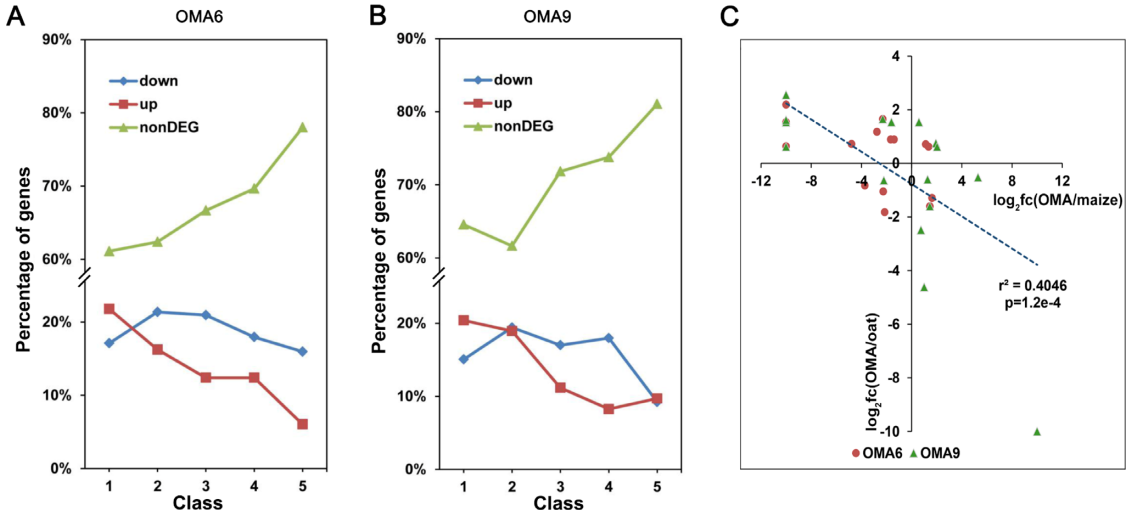

Figure 5. Sequence similarity of maize–oat orthologous pairs shows a positive correlation with the proportion of DEGs. (**A** and **B**) The relative proportion of up- and downregulated genes and non-DEGs show a consistent pattern in (A) OMA6 and (B) OMA9. All expressed genes on the corresponding chromosomes were equally divided into five classes sorted by sequence similarity of maize–oat orthologs. Class 1 contains the orthologs with the highest similarity while Class 5 represents the lowest similarity. The sequence similarity was calculated by bit score analysis using BLAST for the maize genes against the assembled oat transcriptome as well as publicly EST sequences. The oat transcript assigned the highest bit score of each maize gene was defined as the closest corresponding ortholog. (**C**) The fold change of oat transcripts showed a negative correlation with that of maize orthologs.

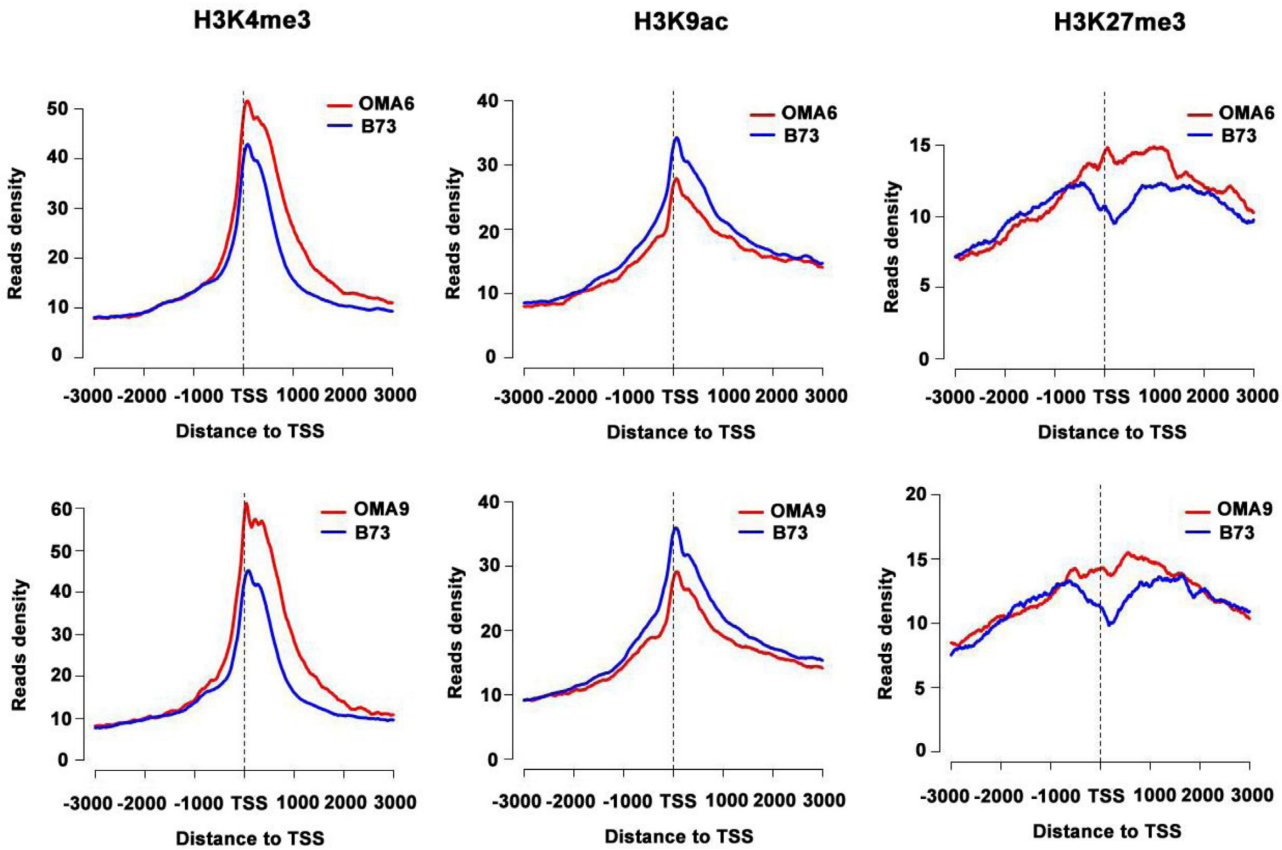

Figure 6. Chromosome-wide distribution of H3K4me3, H3K9ac and H3K27me3 around TSSs. The *x*-axis represents aligned genes, including 3 kb up- and downstream regions from the TSSs, and the *y*-axis represents the density of normalized reads for the three histone modifications. Red lines represent OMA lines, and blue lines represent maize B73. The upper panels represent OMA6 and the lower panels denote OMA9.

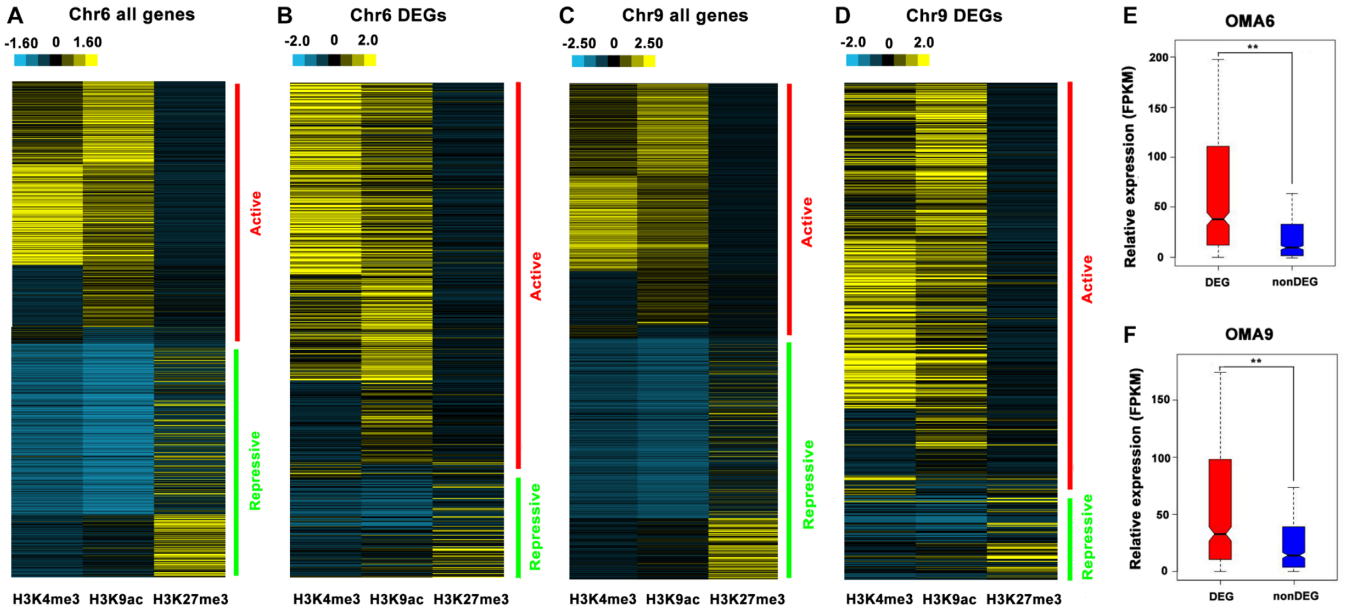

Figure 7. DEGs were over-represented among actively transcriptional genes. (**A** and **C**) A heatmap clustered by ChIP-seq signals for H3K4me3, H3K9ac and H3K27me3 for all genes in Chr6 (A) and Chr9 (C). (**B** and **D**) A heatmap clustered by ChIP-seq signals of H3K4me3, H3K9ac and H3K27me3 for DEGs in OMA6 (B) and OMA9 (D). The scale of color density correlates with the $\log_2$ value of ChIP-seq signal fold changes in genes. (**E** and **F**) Comparison between the expression level of DEGs and non-DEGs in B73 leaves. $^{**}P < 0.005$ according to a Wilcoxon rank-sum test.

To further investigate the effects of the chromatin modifications on gene expression in OMAs, we compared the extent of histone modification on the DEGs in the B73 versus the OMAs. The OMA6 and OMA9 presented similar patterns of all three profiled modifications. Specifically, the upregulated genes showed considerably more H3K4me3 modification in the OMAs than in the B73, whereas showed no evident change in the H3K9ac modification in the OMAs and B73 (Figure 8), indicating that H3K4me3 may be associated with gene upregulation but H3K9ac may not. The DEGs mainly comprised highly expressed genes (Figure 7 E and F). Similar to our findings, previous studies also showed that in highly abundant transcripts, H3K4me3 may be better correlated to gene expression than H3K9ac (49,50). The downregulated genes had substantially lower H3K9ac levels in the OMAs than in the B73, and showed slightly lower H3K4me3 levels in the OMA6 and unchanged H3K4me3 levels in the OMA9 compared with those in the B73 (Figure 8). These results indicate that transcriptional upregulation may be associated with increased H3K4me3 while transcriptional downregulation may be accompanied with reduced H3K9ac modification in OMA lines. Notably, both up- and downregulated DEGs showed higher H3K27me3 levels in the OMA lines than in the B73 (Figure 8), indicating that this modification may contribute to inactivation of the alien maize chromosome in the oat genetic environment. There are likely many other histone modifications that could contribute to the regulation of the alien maize chromosome. Neither maize Chr6 nor Chr9 encode their own maize histone modification machinery in OMAs. Hence, oat epigenetic machinery is responsible for the corresponding alien maize chromosome histone modifications.

The expanded centromere regions were epigenetically and transcriptionally activated in OMA

Centromere chromatin is assembled by a discontinuous subdomain that is occupied by the centromeric H3 (CENH3) variant. The intervals between the discontinuous subdomain are filled by the canonical H3, which is commonly modified by H3K9ac, H3K4me3, H3K36me3, and et cetera, and the centromere interval is typically associated with infrequent zones of transcriptional activation (51,52). The maize *CenH3* gene (GRMZM2G158526) on Chr6 was significantly downregulated in the OMA6 (with FPKM = 9.07425 in the maize B73 in contrast to FPKM = 1.87628 in the OMA6) and showed elevated H3K27me3 (Supplementary Figure S6). The suppression of the maize *CenH3* gene in the oat genomic environment is consistent with previous findings also showing silenced alien *CenH3* in distant hybridization (53,54).

Centromere chromatin is interspersed with partially active subdomains, while the pericentromeric region usually comprises condensed heterochromatin and inactive genes (55). A recent study analyzed maize addition chromosomes by CENH3-ChIP-seq and found that the centromere was expanded in the OMA, consequently causing the centromere to acquire a new flanking border, which was originally part of the pericentromere (56). To investigate the effects of centromere expansion on maize gene expression in OMA, we analyzed gene activity in the newly expanded centromere. These regions were previously defined as 47.7–50.1 Mb and 53.1–55.1 Mb on Chr6 and Chr9, respectively, based on the CENH3-ChIP-seq assay (Figure 9A and B) (56). Overall, 20 and 19 annotated genes were found in the new centromere of OMA6 and OMA9, respectively, of which, 10 genes in OMA6 and 12 genes in OMA9 were silenced (FPKM = 0) in both B73 and

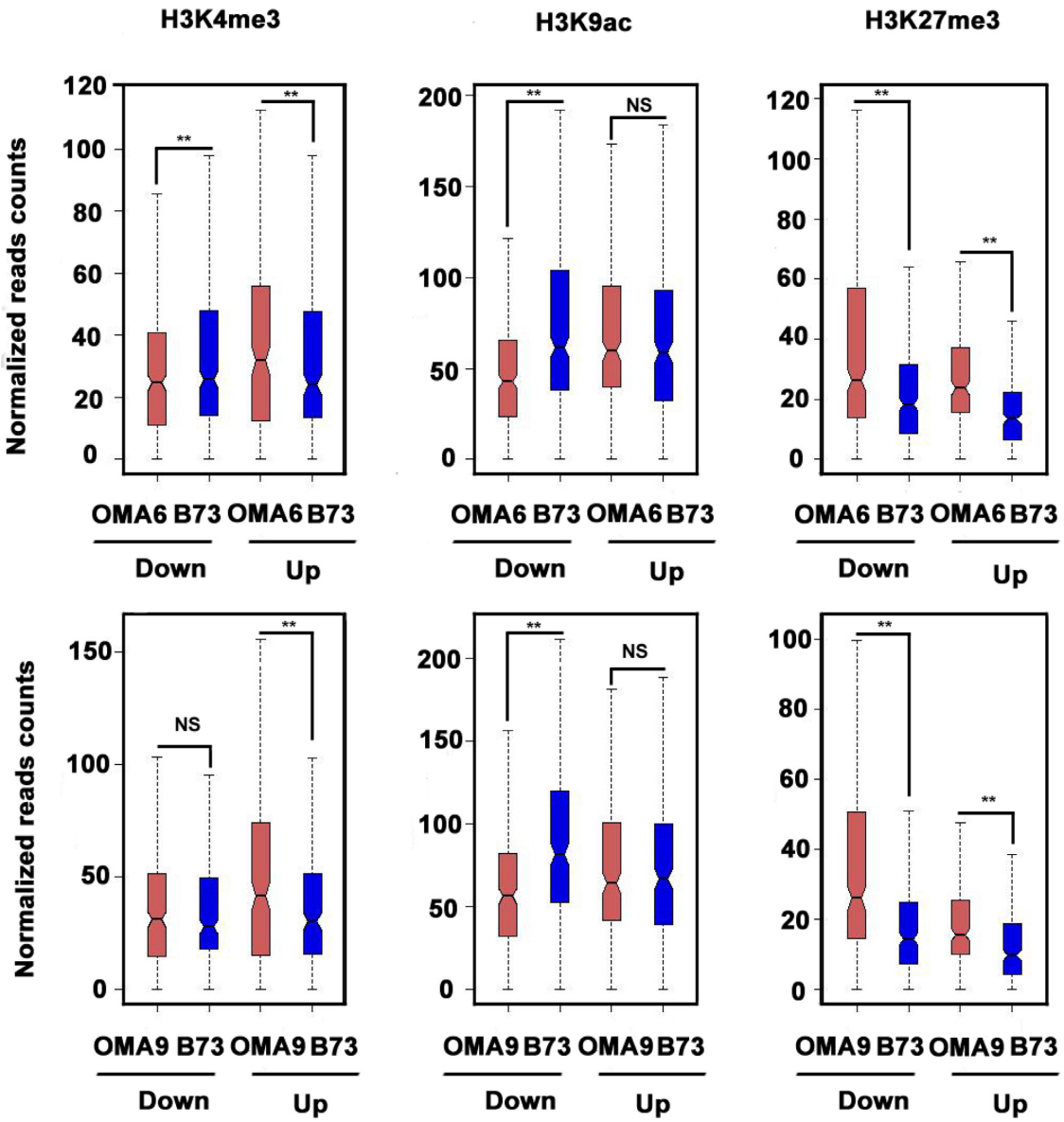

Figure 8. Correlation pattern of DEGs with histone modifications. Comparison of the normalized ChIP-seq signal of H3K4me3, H3K9ac and H3K27me3 for up- and downregulated genes in OMA and maize B73, respectively. Red boxplots correspond to the density of ChIP-seq normalized reads of OMA lines and blue boxplots represent the density of normalized reads of maize B73. The top track represents OMA6 and the bottom track represents OMA9. **A significant difference according to a Wilcoxon rank-sum test. NS: Not significant.

the OMA line. These results indicate that the newly expanded centromeres may be similar to the normal centromere or percentromere in terms of low transcriptional activity. Of the 17 expressed genes (10 from the OMA6 and 7 from the OMA9) from the expanded centromere, four were upregulated significantly (FPKM increased from 0 to 96.89 for AC187279.3_FG004, from 5.23 to 23.91 for GRMZM2G154422 in OMA6; and FPKM increased from 2.09 to 39.35 for GRMZM2G162675, and from 0.61 to 34.51 for GRMZM2G097983 in OMA9); none was downregulated significantly in either OMA6 or OMA9 (Supplementary Table S10). In addition, when only considering fold change of the FPKM values, six genes were upregulated by more than 2-fold and two genes were downregulated by more than 2-fold in the OMA6. In the OMA9, five genes were upregulated by at least 2-fold and no genes were downregulated by more than 2-fold (Figure 9A and B). We used maize-specific primers in qRT–PCR to validate the results from the RNA-seq assay and found substantial upregulation of gene transcription (Supplementary Figure S7). In contrast, we detected transcriptional repression in the 3-Mb pericentromere region adjacent to the newly expanded centromere border, showing three up- and nine downregulated genes in the OMA6 and six up- and nine downregulated genes in the OMA9 (Figure 9A and B; Supplementary Table S10). These data indicate that expanded centromere chromatin may activate the gene transcription that was suppressed by the original pericentromere (56,57).

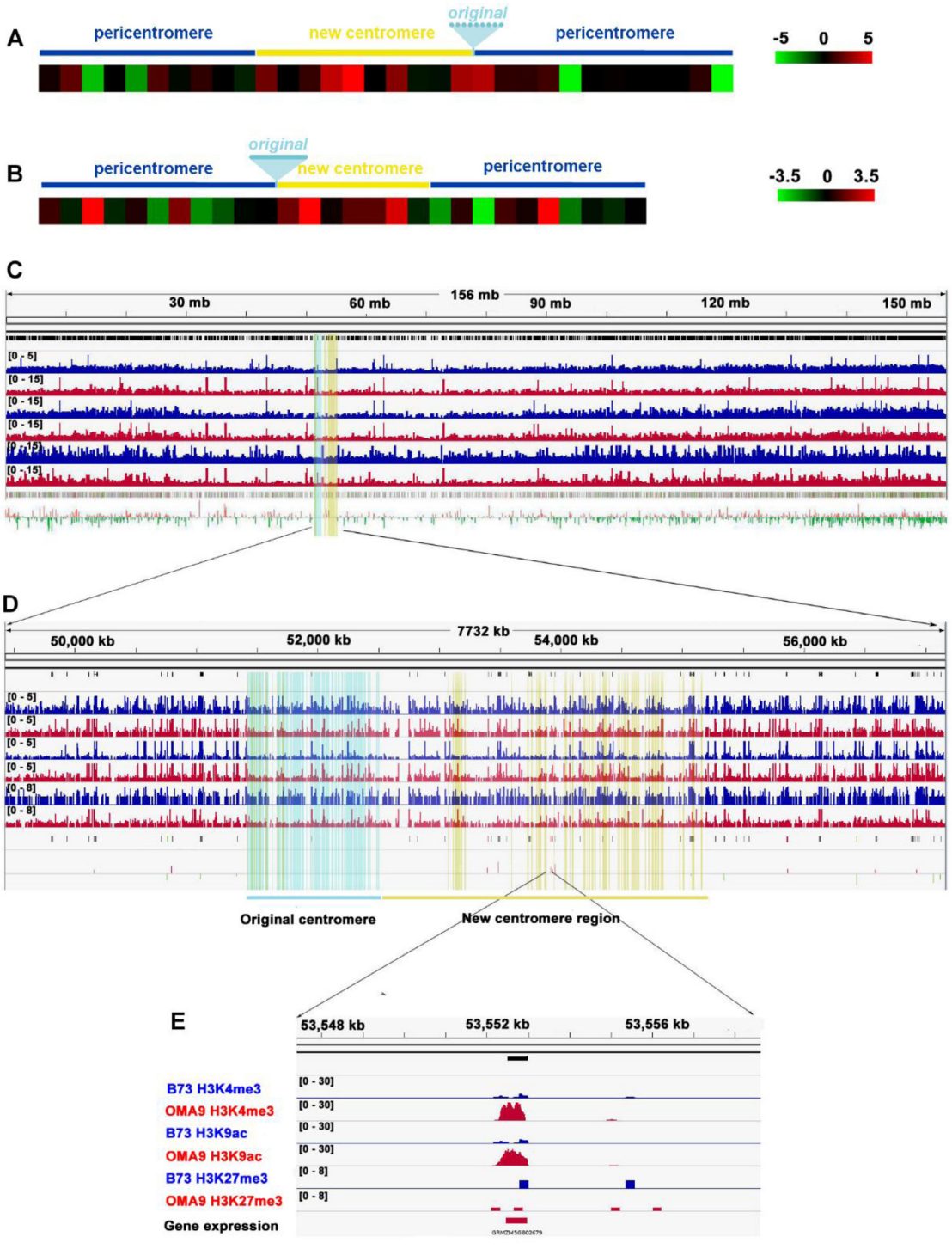

Figure 9. New centromeric genes were activated but the genes in the surrounding region were not. (**A** and **B**) Profile of the gene expression in the newly expanded centromere and surrounding pericentromere. Only genes with FPKM > 1 were used in this analysis. The new centromere (yellow shaded region) was defined as the previous description (56) by CENH3 ChIP-seq in maize and OMA lines, and the surrounding, ∼3 Mb pericentromere region (dark blue shaded region) was also used in this comparison. Original maize centromeric genes were not displayed in this figure because the maize centromere on Chr6 was not accurately defined (light blue dotted line in A) (56), and no gene showed an FPKM value >1 in the Chr9 original centromeric region (light blue line in B). The scale of color density correlates with the $\log_2$ value of the fold change in genes. Overwhelming upregulation occurred among the newly centromeric genes, in contrast to the observation of downregulated genes in the pericentromeric region. (**C** and **D**) Profiles of transcription and histone modifications throughout the chromosome (C) and centromere region (D). Blue shading represents the original centromere region, and yellow shading represents the new centromere region. Blue bars in rows 1, 3 and 5 represent maize H3K4me3, H3K9ac and H3K27me3, respectively; red bars in rows 2, 4, 6 stand for OMA H3K4me3, H3K9ac and H3K27me3, respectively. The last row represents gene expression. Red, green and gray bars represent upregulated, downregulated and unchanged genes, respectively. (**E**) Profiles of transcription and histone modifications for gene model GRMZM5G802679, which was significantly induced in OMA9.

The majority of the genes from the expanded centromere are in a CENH3-depleted subdomain, which is occupied by canonical H3 (56), and the canonical H3 can be modified so to regulate transcriptional activation. Concurrent with the transcriptional activation in the expanded centromere of the OMA6 and OMA9, epigenetic modifications were also observed in the upregulated genes (Figure 9C and D; Supplementary Figure S8A). For example, AC187279.3_FG004 from Chr6 and GRMZM5G802679 from Chr9 were identified as significantly upregulated genes in the newly expanded centromere; both showed increased H3K4me3 and H3K9ac around the TSS and reduced H3K27me3 (Figure 9E and Supplementary Figure S8B). These finding suggest an association between chromatin modification and gene expression in the newly established centromere and support the hypothesis of antagonistic interaction between gene expression and CENH3 occupation (56).

DISCUSSION

Substantial recapitulations of maize transcription in oat genome

Compared with animals, plants are highly tolerant of interspecies hybridization (3). Most reported plant interspecies hybrids have a polyploid parent, implying that abundant paralogous gene pairs in polyploid genomes may compensate for alien chromosome-mediated genomic imbalance during interspecies hybridization (3,19). Maize is often crossed with related grass species to produce haploids. OMA lines stably inherit one complete paternal maize chromosome after nine of the 10 maize chromosomes are eliminated randomly (Figure 1, (19)). In this artificial germplasm, a pair of diploid chromosomes (maize) has been introduced to an allohexaploid genome (oat). Thus OMA lines ideal models to investigate the mechanism underlying both chromosome survival and adaptation in the recipient genomic environment. In this study, we used high-throughput RNA-seq to analyze the gene transcription of maize addition chromosomes in OMA lines, accounting for transcriptome size differences between the donor maize and the OMA in our analyses. In contrast to the expectation that most genes on the alien chromosome should be silenced in a heterologous genomic environment, we actually found that more than 70% of the genes from the alien maize chromosomes maintained the original expression or transcription pattern under the oat genomic environment (Table 1 and Figure 3A and B). These results are similar to the findings from a previous study, which used microarrays to discover that the gene expression pattern of the human chromosome 21 in aneuploid mouse hepatocytes carrying the human chromosome is largely indistinguishable from that in human hepatocytes (8). Similarly, in plants, gene expression of alien chromosomes has also been detected in OMA lines and wheat–barley addition lines (21,42,58). The preserved gene transcription of the alien addition chromosomes in a heterologous genomic environment in both animals and plants indicates that host transcriptional machinery may be sufficient for alien chromosomes.

Similar to the mutants with lesions resembling diseases, both B73- and Seneca 60-OMA6 lines also develop necrotic leaf blades, and B73- and Seneca 60-OMA9 lines show erratic and premature plant senescence (19,20). These phenotypes may be explained by two mechanisms: (i) some ectopic expression of phenotype-related maize genes may occur under the oat genomic environment; (ii) the interaction between oat and maize transcriptome could change the expression of phenotype-related endogenous oat genes. The second mechanism appears more probable because gain-of-function phenomena are usually rare and we did not identify any apparent gain-of-function expression of phenotype-related genes in our transcriptome analysis. Although an oat genome sequence is currently unavailable, additional studies of the effects of alien maize chromosomes on oat transcriptome in OMA lines could shed light on the underlying mechanism of the OMA phenotypes.

Our results showed that the proportion of DEGs in the total genes on Chr6 was similar to that of DEGs in the total genes of Chr9, as were the proportions of up- and downregulated genes. These findings suggest that different alien maize chromosomes may exhibit similar transcriptional responses to the oat genomic environment. Furthermore, we detected more downregulated than upregulated genes in both OMA6 and OMA9 (Figure 3) and elevated H3K27me3 and reduced H3K9ac on both Chr6 and Chr9 (Figure 6). Nine of the 10 maize chromosomes were randomly eliminated and only one maize chromosome survived in OMAs (19), and although the surviving maize chromosome was not eliminated, the alien maize chromosome in OMAs appears to be somewhat transcriptionally suppressed.

Correlation between conserved coding sequence and non-conserved expression

Similar to the transcriptome of human chromosome in the mouse–human chromosome addition line, the majority (>70%) of the genes on Chr6 and Chr9 inherited their original transcription patterns in the OMA6 and OMA9. Because *cis*-regulatory elements have been considered as the predominant mechanism underlying gene expression in interspecies hybrids and introgressions (15,16,18), we speculated that the maize genes maintaining the original transcription in OMA lines (introgression expression) may be predominantly regulated by a local *cis* element in the alien maize chromosome. Unfortunately, a complete oat genome sequence is unavailable, and we therefore were unable to compare the promoter sequence of the orthologous pairs of oat versus maize. The promoter sequences may contain *cis*-regulatory elements, such as enhancers and TF binding sites. These elements may contribute to the transcriptional regulation of the imported genes.

In contrast to the maize genome, the added chromosome in OMA exposes the same *cis*-regulatory regions under different *trans* effects, namely those *trans* factors from the oat genome. So we propose *trans* regulation by endogenous oat factors, which could recognize and interact with the corresponding *cis* element on the maize chromosome, is the main mechanism responsible for DEGs. In support of this hypothesis, we found a correlation between conserved coding sequences and differential expression; namely, conserved orthologous pairs tend to be more differentially ex-

pressed than non-conserved ones in the OMA lines (Figure 5). DEGs were also over-represented among syntenic genes but underrepresented among non-syntenic genes (Supplementary Figure S5). The conserved and/or syntenic orthologous pairs of maize and oat may also link with even more conserved upstream and downstream sequences around the gene coding region, which usually contain *cis*-regulatory elements. Because almost all the *trans* factors in OMA lines were from the majority oat genome, highly conserved maize TF binding and chromatin modifications sites within and nearby the alien maize genes would resemble the oat orthologs and therefore be regulated by the host oat regulatory machinery. We observed that originally active genes located in open chromatin in maize are more likely to be differentially expressed in OMAs, which is consistent with the idea that open chromatin creates an accessible binding region for the oat *trans* factors. In addition, our ChIP-seq assay revealed that upregulated genes gained H3K4me3, and downregulated genes gained H3K27me3 and depleted H3K9ac (Figure 8), supporting the hypothesis that chromatin modifications may be part of the *trans*-regulatory mechanism from oat. Taken together, the oat *trans* factors may ultimately lead to the maize gene differential transcription in OMAs.

Additional contributors may be involved in the interaction between orthologous maize and oat genes. Compared with distant orthologous pairs, highly closely related orthologous protein pairs, which have highly conserved transcript sequences, may show greater dosage effects (59–63). Our data showed a negative correlation between the fold change in gene expression of maize orthologs and the fold change in oat orthologs (Figure 5), indicating mutual compensation between maize and oat orthologous transcripts.

Transcriptional and epigenetic activation in the expanded centromere

The CENH3 binding regions of maize chromosomes were expanded in OMA lines, forming new centromere regions in the original pericentromeres (56). In the current study, we compared the new centromeric transcription of the OMA lines versus the original maize centromeric transcription and found strong gene activation in the new centromere. Furthermore, the upregulated genes in this region were accompanied by elevated levels of the euchromatin markers, H3K4me3 and H3K9ac (Figure 8 and Supplementary Figure S8), reflecting a similar correlation between gene expression and chromatin modification as in endogenous maize euchromatin. The increases in H3K4me3 and H3K9ac in centromeric genes has also been observed in rice (52). In contrast, both H3K4me3 and H3K9ac were depleted from the centromeric interspersed H3 in humans and *Drosophila melanogaster* (64), implying different epigenetic regulation of the centromeric transcription in plants and animals. The animal core centromere contains satellite DNA whereas plant centromere contains a number of genes interspersed in the CENH3-depleted subdomains (65). Besides histone modifications, DNA methylation could be another important contributing factors to be involved in the centromeric expression. Nevertheless, the cause-effect relationship between epigenetic modification and centromeric transcription in animals and plants needs to be further investigated.

In contrast to the gene activation by the expanded CENH3, no gene activation was observed in the surrounding pericentromeres. Centromeric transcription may be important for centromere stability (66). Thus, gene activation in the centromere and the inactivation in the pericentromere may contribute to the identification of the core centromere boundary, which ensures an appropriate mitotic and meiotic division in interspecific hybrid or polyploid.

DATA AVAILABILITY

Sequence data from this article can be found in the NCBI Short Read Archive sequence database under Accession Number SRP080643.

SUPPLEMENTARY DATA

Supplementary Data are available at NAR Online.

ACKNOWLEDGEMENTS

We are grateful to Dr James Birchler, Dr Xiangfeng Wang and Samuel Leiboff for critically reading and commenting on our manuscript. We thank Dr Howard W. Rines and Dr Ronald L. Phillips for OMA seeds.
Authors' contributions: W.J. and Z.S. designed and supervised the project. Z.D., H.L. and W.H. performed the experiments. Z.D., J.Y. and L.X carried out the data analysis. Y.Z., T.Z., W. X. and J.J. assisted in analyzing the data. Z.D. and W.J. wrote the article.

FUNDING

National Natural Science Foundation of China [31421005, 91735305 to W.J., 31371291 to Z.S.]; National Science Foundation [IOS-1444514 to J.J.]. Funding for open access charge: National Natural Science Foundation of China [31421005].
Conflict of interest statement. None declared.

REFERENCES

1. Song,Q. and Chen,Z.J. (2015) Epigenetic and developmental regulation in plant polyploids. *Curr. Opin. Plant Biol.*, **24**, 101–109.
2. Leitch,A. and Leitch,I. (2008) Genomic plasticity and the diversity of polyploid plants. *Science*, **320**, 481–483.
3. Maheshwari,S. and Barbash,D.A. (2011) The genetics of hybrid incompatibilities. *Annu. Rev. Genet.*, **45**, 331–355.
4. Ravi,M. and Chan,S.W. (2010) Haploid plants produced by centromere-mediated genome elimination. *Nature*, **464**, 615–618.
5. Sanei,M., Pickering,R., Kumke,K., Nasuda,S. and Houben,A. (2011) Loss of centromeric histone H3 (CENH3) from centromeres precedes uniparental chromosome elimination in interspecific barley hybrids. *Proc. Natl. Acad. Sci. U.S.A.*, **108**, E498–E505.
6. Forster,B.P., Heberle-Bors,E., Kasha,K.J. and Touraev,A. (2007) The resurgence of haploids in higher plants. *Trends Plant Sci.*, **12**, 368–375.
7. Quiros,C.F., Ochoa,O., Kianian,S.F. and Douches,D. (1987) Analysis of the Brassica oleracea genome by the generation of B. campestris-oleracea chromosome addition lines: characterization by isozymes and rDNA genes. *Theor. Appl. Genet.*, **74**, 758–766.

8. Wilson,M.D., Barbosa-Morais,N.L., Schmidt,D., Conboy,C.M., Vanes,L., Tybulewicz,V.L., Fisher,E.M., Tavare,S. and Odom,D.T. (2008) Species-specific transcription in mice carrying human chromosome 21. *Science*, **322**, 434–438.
9. Islam,A., Shepherd,K. and Sparrow,D. (1981) Isolation and characterization of euplasmic wheat-barley chromosome addition lines. *Heredity*, **46**, 161–174.
10. Chen,Y., Wang,Y., Wang,K., Zhu,X., Guo,W., Zhang,T. and Zhou,B. (2014) Construction of a complete set of alien chromosome addition lines from Gossypium australe in Gossypium hirsutum: morphological, cytological, and genotypic characterization. *Theor. Appl. Genet.*, **127**, 1105–1121.
11. Ananiev,E.V., Riera-Lizarazu,O., Rines,H.W. and Phillips,R.L. (1997) Oat-maize chromosome addition lines: a new system for mapping the maize genome. *Proc. Natl. Acad. Sci. U.S.A.*, **94**, 3524–3529.
12. Alkhimova,A.G., Heslop-Harrison,J.S., Shchapova,A.I. and Vershinin,A.V. (1999) Rye chromosome variability in wheat-rye addition and substitution lines. *Chromosome Res.*, **7**, 205–212.
13. Wittkopp,P.J. and Kalay,G. (2012) Cis-regulatory elements: molecular mechanisms and evolutionary processes underlying divergence. *Nat. Rev. Genet.*, **13**, 59–69.
14. Wittkopp,P.J., Haerum,B.K. and Clark,A.G. (2008) Regulatory changes underlying expression differences within and between Drosophila species. *Nat. Genet.*, **40**, 346–350.
15. Tirosh,I., Reikhav,S., Levy,A.A. and Barkai,N. (2009) A yeast hybrid provides insight into the evolution of gene expression regulation. *Science*, **324**, 659–662.
16. Shi,X., Ng,D.W., Zhang,C., Comai,L., Ye,W. and Chen,Z.J. (2012) Cis- and trans-regulatory divergence between progenitor species determines gene-expression novelty in Arabidopsis allopolyploids. *Nat. Commun.*, **3**, 950.
17. Romero,I.G., Ruvinsky,I. and Gilad,Y. (2012) Comparative studies of gene expression and the evolution of gene regulation. *Nat. Rev. Genet.*, **13**, 505–516.
18. Koenig,D., Jimenez-Gomez,J.M., Kimura,S., Fulop,D., Chitwood,D.H., Headland,L.R., Kumar,R., Covington,M.F., Devisetty,U.K., Tat,A.V. *et al.* (2013) Comparative transcriptomics reveals patterns of selection in domesticated and wild tomato. *Proc. Natl. Acad. Sci. U.S.A.*, **110**, E2655–E2662.
19. Kynast,R.G., Riera-Lizarazu,O., Vales,M.I., Okagaki,R.J., Maquieira,S.B., Chen,G., Ananiev,E.V., Odland,W.E., Russell,C.D., Stec,A.O. *et al.* (2001) A complete set of maize individual chromosome additions to the oat genome. *Plant Physiol.*, **125**, 1216–1227.
20. Rines,H.W., Phillips,R.L., Kynast,R.G., Okagaki,R.J., Galatowitsch,M.W., Huettl,P.A., Stec,A.O., Jacobs,M.S., Suresh,J., Porter,H.L. *et al.* (2009) Addition of individual chromosomes of maize inbreds B73 and Mo17 to oat cultivars Starter and Sun II: maize chromosome retention, transmission, and plant phenotype. *Theor. Appl. Genet.*, **119**, 1255–1264.
21. Cho,S., Garvin,D.F. and Muehlbauer,G.J. (2006) Transcriptome analysis and physical mapping of barley genes in wheat–barley chromosome addition lines. *Genetics*, **172**, 1277–1285.
22. Rajhathy,T and Morrison,J.W. (1959) Chromosome morphology in the genus *Avena*. *Canadian Journal of Botany*, **37**, 331–337.
23. Thomas,H. (1992) Cytogenetics of *Avena*. In: Marshall,HG and Sorrells,ME (eds). *Oat Science and Technology*. American Society of Agronomy and Crop Science Society of America. Madison, Vol. **33**, pp. 473–507.
24. Chew,P., Meade,K., Hayes,A., Harjes,C., Bao,Y., Beattie,A.D., Puddephat,I., Gusmini,G. and Tanksley,S.D. (2016) A study on the genetic relationships of Avena taxa and the origins of hexaploid oat. *Theor. Appl. Genet.*, **129**, 1405–1415.
25. Jiang,J., Gill,B.S., Wang,G.L., Ronald,P.C. and Ward,D.C. (1995) Metaphase and interphase fluorescence in situ hybridization mapping of the rice genome with bacterial artificial chromosomes. *Proc. Natl. Acad. Sci. U.S.A.*, **92**, 4487–4491.
26. Zhao,X., Lu,J., Zhang,Z., Hu,J., Huang,S. and Jin,W. (2011) Comparison of the distribution of the repetitive DNA sequences in three variants of Cucumis sativus reveals their phylogenetic relationships. *J. Genet. Genomics*, **38**, 39–45.
27. Wang,G., He,Q., Liu,F., Cheng,Z., Talbert,P.B. and Jin,W. (2011) Characterization of CENH3 proteins and centromere-associated DNA sequences in diploid and allotetraploid Brassica species. *Chromosoma*, **120**, 353–365.
28. Du,Z., Li,H., Wei,Q., Zhao,X., Wang,C., Zhu,Q., Yi,X., Xu,W., Liu,X.S., Jin,W. *et al.* (2013) Genome-wide analysis of histone modifications: H3K4me2, H3K4me3, H3K9ac, and H3K27ac in Oryza sativa L. Japonica. *Mol. Plant*, **6**, 1463–1472.
29. Dong,Z., Jiang,C., Chen,X., Zhang,T., Ding,L., Song,W., Luo,H., Lai,J., Chen,H., Liu,R. *et al.* (2013) Maize LAZY1 mediates shoot gravitropism and inflorescence development through regulating auxin transport, auxin signaling, and light response. *Plant Physiol.*, **163**, 1306–1322.
30. Coate,J.E. and Doyle,J.J. (2010) Quantifying whole transcriptome size, a prerequisite for understanding transcriptome evolution across species: an example from a plant allopolyploid. *Genome Biol. Evol.*, **2**, 534–546.
31. Trapnell,C., Pachter,L. and Salzberg,S.L. (2009) TopHat: discovering splice junctions with RNA-Seq. *Bioinformatics*, **25**, 1105–1111.
32. Grabherr,M.G., Haas,B.J., Yassour,M., Levin,J.Z., Thompson,D.A., Amit,I., Adiconis,X., Fan,L., Raychowdhury,R., Zeng,Q. *et al.* (2011) Full-length transcriptome assembly from RNA-Seq data without a reference genome. *Nat. Biotechnol.*, **29**, 644–652.
33. Trapnell,C., Roberts,A., Goff,L., Pertea,G., Kim,D., Kelley,D.R., Pimentel,H., Salzberg,S.L., Rinn,J.L. and Pachter,L. (2012) Differential gene and transcript expression analysis of RNA-seq experiments with TopHat and Cufflinks. *Nat. Protoc.*, **7**, 562–578.
34. Du,Z., Zhou,X., Ling,Y., Zhang,Z. and Su,Z. (2010) agriGO: a GO analysis toolkit for the agricultural community. *Nucleic Acids Res.*, **38**, W64–W70.
35. Ye,J., McGinnis,S. and Madden,T.L. (2006) BLAST: improvements for better sequence analysis. *Nucleic Acids Res.*, **34**, W6–W9.
36. Langmead,B. and Salzberg,S.L. (2012) Fast gapped-read alignment with Bowtie 2. *Nat. Methods*, **9**, 357–359.
37. Zhang,Y., Liu,T., Meyer,C.A., Eeckhoute,J., Johnson,D.S., Bernstein,B.E., Nusbaum,C., Myers,R.M., Brown,M., Li,W. *et al.* (2008) Model-based Analysis of ChIP-Seq (MACS). *Genome Biol.*, **9**, R137.
38. Robinson,J.T., Thorvaldsdóttir,H., Winckler,W., Guttman,M., Lander,E.S., Getz,G. and Mesirov,J.P. (2011) Integrative genomics viewer. *Nat. Biotechnol.*, **29**, 24–26.
39. Shin,H., Liu,T., Manrai,A.K. and Liu,X.S. (2009) CEAS: cis-regulatory element annotation system. *Bioinformatics*, **25**, 2605–2606.
40. Chia,J.M., Song,C., Bradbury,P.J., Costich,D., de Leon,N., Doebley,J., Elshire,R.J., Gaut,B., Geller,L., Glaubitz,J.C. *et al.* (2012) Maize HapMap2 identifies extant variation from a genome in flux. *Nat. Genet.*, **44**, 803–807.
41. Gore,M.A., Chia,J.-M., Elshire,R.J., Sun,Q., Ersoz,E.S., Hurwitz,B.L., Peiffer,J.A., McMullen,M.D., Grills,G.S. and Ross-Ibarra,J. (2009) A first-generation haplotype map of maize. *Science*, **326**, 1115–1117.
42. Kowles,R., Walch,M., Minnerath,J., Bernacchi,C., Stec,A., Rines,H. and Phillips,R. (2008) Expression of C4 photosynthetic enzymes in oat-maize chromosome addition lines. *Maydica*, **53**, 69.
43. Tolley,B.J., Sage,T.L., Langdale,J.A. and Hibberd,J.M. (2012) Individual maize chromosomes in the C(3) plant oat can increase bundle sheath cell size and vein density. *Plant Physiol.*, **159**, 1418–1427.
44. Pérez-Rodríguez,P., Riano-Pachon,D.M., Correa,L.G., Rensing,S.A., Kersten,B. and Mueller-Roeber,B. (2010) PlnTFDB: updated content and new features of the plant transcription factor database. *Nucleic Acids Res.*, **38**, D822–D827.
45. Cheng,F., Wu,J., Fang,L., Sun,S., Liu,B., Lin,K., Bonnema,G. and Wang,X. (2012) Biased gene fractionation and dominant gene expression among the subgenomes of Brassica rapa. *PLoS One*, **7**, e36442.
46. Freeling,M., Woodhouse,M.R., Subramaniam,S., Turco,G., Lisch,D. and Schnable,J.C. (2012) Fractionation mutagenesis and similar consequences of mechanisms removing dispensable or less-expressed DNA in plants. *Curr. Opin. Plant Biol.*, **15**, 131–139.
47. Schnable,J.C., Springer,N.M. and Freeling,M. (2011) Differentiation of the maize subgenomes by genome dominance and both ancient and ongoing gene loss. *Proc.e Natl. Acad. Sci. U.S.A.*, **108**, 4069–4074.
48. Woodhouse,M.R., Schnable,J.C., Pedersen,B.S., Lyons,E., Lisch,D., Subramaniam,S. and Freeling,M. (2010) Following tetraploidy in

maize, a short deletion mechanism removed genes preferentially from one of the two homologs. *PLoS Biol.*, **8**, e1000409.
49. Wang,X., Elling,A.A., Li,X., Li,N., Peng,Z., He,G., Sun,H., Qi,Y., Liu,X.S. and Deng,X.W. (2009) Genome-wide and organ-specific landscapes of epigenetic modifications and their relationships to mRNA and small RNA transcriptomes in maize. *Plant Cell*, **21**, 1053–1069.
50. Ha,M., Ng,D.W., Li,W.H. and Chen,Z.J. (2011) Coordinated histone modifications are associated with gene expression variation within and between species. *Genome Res.*, **21**, 590–598.
51. Hall,L.E., Mitchell,S.E. and O'Neill,R.J. (2012) Pericentric and centromeric transcription: a perfect balance required. *Chromosome Res.*, **20**, 535–546.
52. Wu,Y., Kikuchi,S., Yan,H., Zhang,W., Rosenbaum,H., Iniguez,A.L. and Jiang,J. (2011) Euchromatic subdomains in rice centromeres are associated with genes and transcription. *Plant Cell*, **23**, 4054–4064.
53. Chen,W., Zhu,Q., Wang,H., Xiao,J., Xing,L., Chen,P., Jin,W. and Wang,X.E. (2015) Competitive expression of endogenous wheat CENH3 may lead to suppression of alien ZmCENH3 in transgenic wheat x maize hybrids. *J. Genet. Genomics*, **42**, 639–649.
54. Jin,W., Melo,J.R., Nagaki,K., Talbert,P.B., Henikoff,S., Dawe,R.K. and Jiang,J. (2004) Maize centromeres: organization and functional adaptation in the genetic background of oat. *Plant Cell*, **16**, 571–581.
55. Ananiev,E.V., Phillips,R.L. and Rines,H.W. (2000) Complex structure of knobs and centromeric regions in maize chromosomes. *Tsitol. Genet.*, **34**, 11–15.
56. Wang,K., Wu,Y., Zhang,W., Dawe,R.K. and Jiang,J. (2014) Maize centromeres expand and adopt a uniform size in the genetic background of oat. *Genome Res.*, **24**, 107–116.
57. Zhao,H., Zhu,X., Wang,K., Gent,J.I., Zhang,W., Dawe,R.K. and Jiang,J. (2016) Gene expression and chromatin modifications associated with maize centromeres. *G3*, **6**, 183–192.
58. Muehlbauer,G., Riera-Lizarazu,O., Kynast,R., Martin,D., Phillips,R. and Rines,H. (2000) A maize chromosome 3 addition line of oat exhibits expression of the maize homeobox gene liguleless3 and alteration of cell fates. *Genome*, **43**, 1055–1064.
59. Birchler,J.A. and Veitia,R.A. (2012) Gene balance hypothesis: connecting issues of dosage sensitivity across biological disciplines. *Proc. Natl. Acad. Sci. U.S.A.*, **109**, 14746–14753.
60. Birchler,J.A. and Veitia,R.A. (2011) Protein-protein and protein-DNA dosage balance and differential paralog transcription factor retention in polyploids. *Front. Plant Sci.*, **2**, 64.
61. Yao,H., Dogra Gray,A., Auger,D.L. and Birchler,J.A. (2013) Genomic dosage effects on heterosis in triploid maize. *Proc. Natl. Acad. Scie. U.S.A.*, **110**, 2665–2669.
62. Guo,M. and Birchler,J.A. (1994) Trans-acting dosage effects on the expression of model gene systems in maize aneuploids. *Science*, **266**, 1999–2002.
63. Schnable,J.C., Pedersen,B.S., Subramaniam,S. and Freeling,M. (2011) Dose-sensitivity, conserved non-coding sequences, and duplicate gene retention through multiple tetraploidies in the grasses. *Front. Plant Sci.*, **2**, 2.
64. Sullivan,B.A. and Karpen,G.H. (2004) Centromeric chromatin exhibits a histone modification pattern that is distinct from both euchromatin and heterochromatin. *Nat. Struct. Mol. Biol.*, **11**, 1076–1083.
65. McKinley,K.L. and Cheeseman,I.M. (2016) The molecular basis for centromere identity and function. *Nat. Rev. Mol. Cell Biol.*, **17**, 16–29.
66. Lermontova,I., Sandmann,M., Mascher,M., Schmit,A.C. and Chaboute,M.E. (2015) Centromeric chromatin and its dynamics in plants. *Plant J.*, **83**, 4–17.